Figure S4

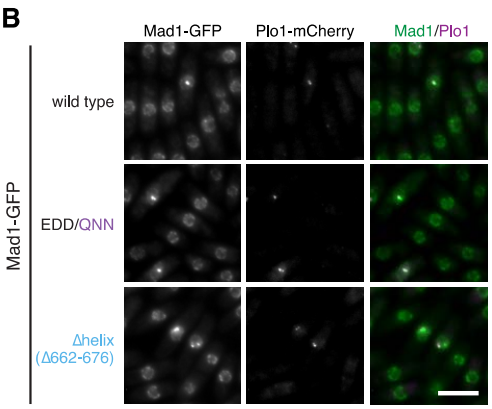
B
Mad1-GFP
Plo1-mCherry
Mad1/Plo1
Mad1-GFP
wild type
EDD/QNN
Δhelix
(Δ662-676)

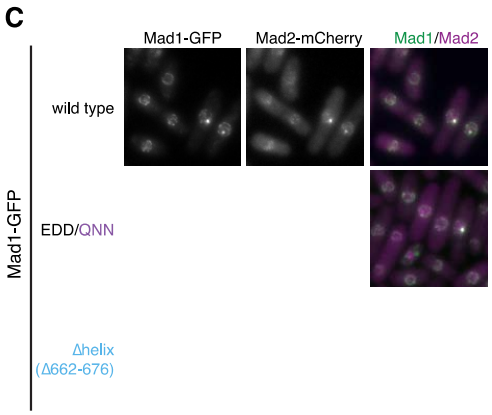
C
Mad1-GFP
Mad2-mCherry
Mad1/Mad2
Mad1-GFP
wild type
EDD/QNN
Δhelix
(Δ662-676)

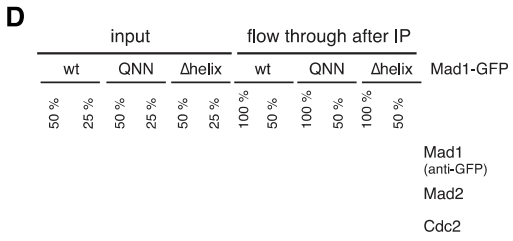
D
input
flow through after IP
wt
QNN
Δhelix
wt
QNN
Δhelix
Mad1-GFP
50 %
25 %
50 %
25 %
50 %
25 %
100 %
50 %
100 %
50 %
100 %
50 %
Mad1
(anti-GFP)
Mad2
Cdc2


E
F
0000

Figure S4 Supplementary data for C-terminal Mad1 mutants

A Additional Mad1 mutants screened for kinetochore targeting ability and spindle assembly checkpoint activity

Individual residues in Mad1 were mutated to alanine, with the exception of S633, which was mutated to glycine. Checkpoint activity was assayed in cells expressing *plo1+-mCherry* and *nda3-KM311* as in Fig 1F. Mad1 localisation to kinetochores was scored as cells entered mitosis.

B Mad1-EDD/QNN and Mad1-Δhelix show similar localisation to wild type Mad1

Representative images of cells expressing *plo1+-mCherry*, *nda3-KM311* and the indicated *mad1-GFP* fusions. Cells were grown at permissive temperature for the *nda3-KM311* mutant (30 °C). Scale bar: 10 µm

C Mad2-mCherry localisation is not perturbed by *mad1-EDD/QNN* or *mad1-Δhelix*

Representative images of cells expressing *mad2+-mCherry*, *nda3-KM311* and the indicated *mad1-GFP* fusions. Cells were grown at permissive temperature for the *nda3-KM311* mutant (30 °C). Scale bar: 10 µm

D Input and flow through of the anti-Mad1 immunoprecipitation shown in Fig 3F. Cdc2 was used as loading control.

E Statistical analysis of Mad2/Mad1 ratios shown in Fig 3G. Intensity curves of the indicated strains were compared by a pooled component test [3]. The cumulative p-value is plotted in red. A p-value of 0.05 is shown as dashed blue line. Only time points with at least 7 cells of all strains were considered. The experiment index (i) increases with each time point. There is a statistically significant difference between the Mad1-GFP wild type or mutants strains expressing *mad2+-mCherry* and the same strains expressing the Mad2 dimerization mutant *mad2-R133A-mCherry* (upper row), indicating that in both Mad1 mutants Mad2 dimerization is not impaired. Differences between Mad1 wt and Mad1 mutant strains expressing wild type *mad2+-mCherry* were not statistically significant (lower row).

F Statistical analysis of Mad2/Mad1 ratios shown in Fig 3H. Intensity curves of the indicated strains were compared by a pooled component test [3] as in (E). There is a statistically significant difference between the Mis12-Mad1-GFP wild type or RLK/AAA strains expressing *mad2+-mCherry* and the Mis12-Mad1-GFP wild type strain expressing the Mad2 dimerization mutant *mad2-R133A-mCherry*. This indicates that Mad2 dimerization in Mis12-Mad1-RLK/AAA-GFP is not impaired.

G Bub1-GFP localisation is not perturbed in untagged *mad1-EDD/QNN* or *mad1-Δhelix* cells

Representative nuclei of cells expressing *bub1+-GFP, plo1+-mCherry*, *nda3-KM311* and the indicated *mad1* variants (wild type, EDD/QNN or Δhelix). Cells were grown at permissive temperature for the *nda3-KM311* mutant (30 °C). Scale bar: 2 µm

H Expression level of untagged *mad1-Δhelix* is reduced compared to *mad1+* and *mad1-EDD/QNN*

Immunoblotting of cell extracts using anti-Mad1 and anti-Cdc2 (loading control) antibodies. The Mad1 antibody targets an N-terminal peptide [4]. Cell extracts of two different clones expressing *mad1-Δhelix* were loaded. Both Mad1 mutants were detectable but Mad1-Δhelix abundance was lower than wild type

Mad1 or Mad1-EDD/QNN abundance. Note that C-terminal GFP-tagging of Mad1-Δhelix seems to rescue protein stability (Fig 3E). Bub1 localisation in all strains was preserved (G).

Supplementary References

3. Wu Y, Genton MG, Stefanski LA (2006) A multivariate two-sample mean test for small sample size and missing data. *Biometrics* **62:** 877-885

4. Heinrich S *et al* (2013) Determinants of robustness in spindle assembly checkpoint signalling. *Nat Cell Biol* **15:** 1328-1339